JOURNAL OF SYNCHROTRON RADIATION

Volume 25 (2018)

Supporting information for article:

Depth dependent atomic valence determination by synchrotron techniques

Robbyn Trappen, Jinling Zhou, Vu Thanh Tra, Chih-Yeh Huang, Shuai Dong, Ying-Hao Chu and Mikel Holcomb

Role of the probing depth in the modeling

The density of the material can have an impact on the probing depth for TEY and there can be variation in its values between systems. In order to determine the implications this has for our model, we ran the fit for a variety of values for the L-edge probing depth. While in the manuscript this value is fixed at 2.6 nm, the figure below shows the fit results for when the probing depth is fixed at different values between the range of 1.5 – 4.5 nm. We believe this range is sufficient to demonstrate the sensitivity of the model due to possible variation in probing depths due to material dependent parameters.

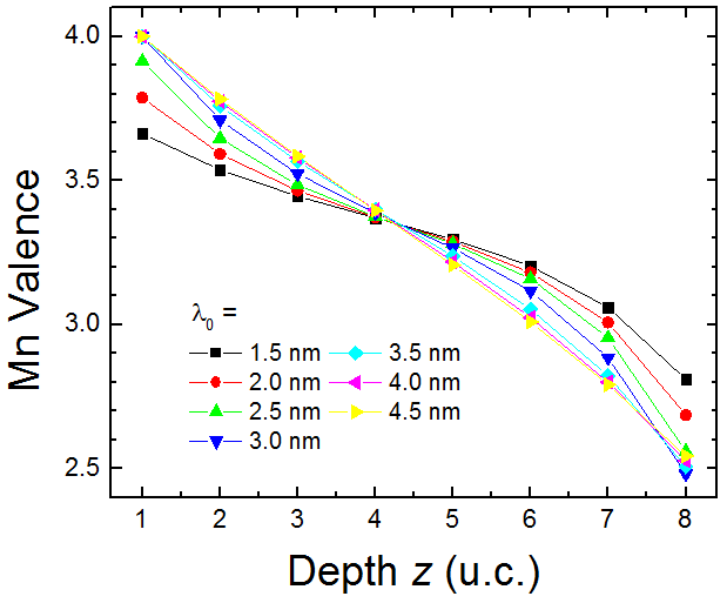

Figure S1. Fitted layer dependent valence for 8 u.c. with the probing depth λ_0 fixed at different values indicated by the legend.

Shown in Figure S1 are the fitted valence profiles for 8 unit cells for each value of the probing depth selected. It can be seen that there is some variation between the profiles, most pronounced at the surface and interface (less so in the bulk of the film) but the overall trend of a raised surface valence and lowered interface valence with similar characteristic lengths of variation can be seen regardless of the value of the probing depth. The overall variation between the surface/interface layer valences between fits is roughly 0.15. We also note that the fits begin to become poor when the probing depth is raised above 3.5 nm. Therefore, the model is most sensitive to the difference in probing depths between the two detection modes and is relatively insensitive to experimental variations of the probing depth.

Power law fits

It is possible that rather than varying exponentially, the valence changes in a power law fashion from its bulk value. To parameterize this change, we introduce the piecewise power-law function

$$P(z,n) = \begin{cases} z^n & z > 0 \\ 0 & z < 0 \end{cases} \quad \text{(S1)}$$

Considering both surface and interface contributions, a similar form to Equation (2) is developed

$$V(z) = \frac{V_{bulk}}{2}\left[1 - \alpha P\left(-(z - L_{surf}), n_{surf}\right)\right] + \frac{V_{bulk}}{2}\left[1 - \beta P(z - (z_{int} - L_{int}), n_{int})\right] \quad \text{(S2)}$$

with the coefficients α and β determined algebraically from the same boundary conditions as before. Figure 6 b) in the main text shows the comparison between the power law variation Equation S2 and the exponential variation Equation (1). In this case, the characteristic length L refers to the distance from the surface/interface where the valence returns to its bulk value, rather than varies by $1/e$ as in the exponential fits.

Fitting was performed similar to those shown in Figure 4 in the main text and are shown in Figure S2. While the fits appears to be reasonable, the obtained fitted values for the parameters L_{int} and n_{int} were 1445.1 ± 198.2 u.c. and 773.8 ± 103.9 respectively. These results with the large error suggest a high degree of coupling between the length scale and power parameters and that the model is likely overfitting the data. Qualitatively, this means that adjusting the length scale and the exponent parameters can create many similar, albeit not identical variations between the material bulk and surface/interface which makes determining the correct variation difficult. For this reason, the exponential variation was chosen instead.

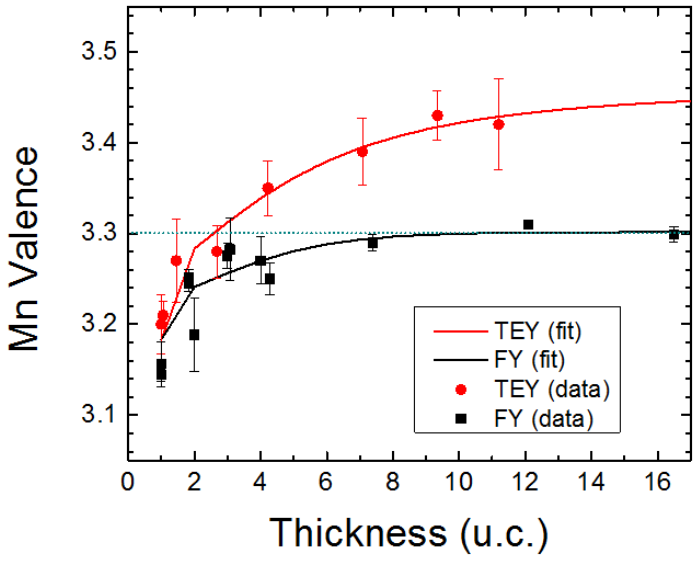

Figure S2. Valence obtained from the linear combination fits (solid points) and best fit using the layer dependent valence model (dashed lines) with the power law variation. The horizontal dashed line indicates the bulk Mn valence for LSMO of 3.3.